Brake Lock Mechanism for the Two Axis Pointing System

Alan Posey*, Mike Clark*, and Larry Mignosa**

ABSTRACT

Six months prior to shipment of the Broad Band X-Ray Telescope to the Kennedy Space Center for flight aboard the space shuttle Columbia, a major system failure occurred. During modal survey testing of the telescope's gimbal pointing system, the roll axis brake unexpectedly released. Low-level vibration and static preloads present during the modal survey were within the expected flight environment. Brake release during shuttle liftoff or ascent was an unacceptable risk to mission success; thus, a Brake Lock Mechanism (BLM) was developed.

INTRODUCTION

The BLM was developed to correct a design problem identified during ground testing of a space shuttle payload. The Broadband X-Ray Telescope (BBXRT) is a Goddard Space Flight Center (GSFC) attached shuttle payload that is part of the National Space Transportation System STS-35 ASTRO-1 Mission, which flew successfully on board the shuttle Columbia in December 1990 (Figure 1). Six months prior to shipment of the payload to the launch site at the Kennedy Space Center, a major system failure occurred. This failure would have resulted in significant loss of BBXRT science if it had occurred during shuttle liftoff or ascent.

The BBXRT payload is composed of three major subsystems: the Two Axis Pointing System (TAPS), the TAPS Support Structure (TSS), and the BBXRT instrument (Figure 2). The TSS is an across-the-bay carrier that supports the TAPS and provides the payload mechanical interface to the shuttle cargo bay. The TAPS supports the BBXRT instrument and provides two axis (roll and pitch) arc minute class pointing capability. The TAPS was built by Space Data Corporation, while the TSS and the BBXRT were built in-house at GSFC.

The TAPS' primary structure consists of an outer gimbal frame, an inner gimbal frame, and two Drive Brake Modules (DBM) as shown in Figure 3. The outer gimbal frame houses the pitch DBM and idler module. The inner gimbal frame

---

* NASA/Goddard Space Flight Center, Greenbelt, MD
** Swales and Associates, Inc., Beltsville, MD

houses the roll DBM and idler module and attaches to the outer frame at the pitch DBM and idler module. The roll axis DBM and idler module are the mechanical interfaces to the BBXRT instrument.

The DBMs restrain the system during shuttle liftoff/ascent and descent/landing events and control system rotation for on-orbit instrument pointing operations. The braking function is accomplished with a rotating gear plate attached to the drive shaft and a translating gear plate restrained in rotation by its tangs and the DBM housing (Figure 4). Each gear plate has 45 teeth that engage every 8 degrees over the normal operating slew range of +/- 20 degrees (Figure 5). The gear teeth have 8 degree sloped sides and a nominal engagement of 2 mm (0.080 in). The translating gear plate is preloaded with four springs to provide positive engagement with the rotating gear plate, thus preventing system rotation. To release the gear plates, power is supplied to a solenoid that retracts the translating gear plate from the rotating plate and holds it there against the force of the springs.

If a TAPS brake were to fail during flight, a Backup Landing Lock (BULL) would safely capture and dissipate the kinetic energy of the freely rotating system. This system failure presents no safety hazards to vehicle or crew. The BULL, however, cannot be released on-orbit and engagement of this backup system would result in significant loss of BBXRT science.

Ground testing at GSFC included a modal survey on the TAPS flight spare unit using low-level mechanical vibration to measure and record its structural dynamic characteristics. A static torsional preload was applied to each DBM to remove nonlinear system responses generated by backlash in the translating gear plate. Under the combined torsional static preload and low-level axial vibration loads, the inner frame brake unexpectedly disengaged and the freely rotating system was captured in the BULL. Since these applied loads were similar in nature to the Space Transportation System (STS) flight environment, it was evident that this failure could occur during shuttle liftoff or ascent.

A TAPS brake failure during shuttle liftoff or ascent was an unacceptable risk to mission success and a hardware change was required. Payload development and launch schedule constraints would not allow DBM disassembly. The design fix had to be accomplished on the TAPS flight unit with the payload in the full-up flight configuration and without disruption to payload Integration and Test activities.

A multi-phase recovery plan was implemented to investigate and determine the cause of the brake failure, to design a mechanism that would preclude unintentional brake release, and to qualify the mechanism for STS flight. The DBM is a large mechanism located in the primary structural load path. Tests and analyses performed to understand the failure demonstrated the sensitivity of DBM gear plate motion to simultaneously applied static and dynamic loading conditions. This implied that flight level static and dynamic loads had to be applied

simultaneously to properly qualify the mechanism.

INVESTIGATION OF BRAKE RELEASE

A Phase 1 test program was developed and executed to determine the cause of the brake release. Phase 1 tests were performed with TAPS in the modal survey facility using a range of flight-like static torques between 339 N-m (3000 in-lb) and 2260 N-m (20,000 in-lb) applied to both the inner and outer frame DBMs. Low-level dynamic axial loads were applied as a sinusoidal sweep. Motion of the translating gear plates was monitored throughout the test. Results for the inner frame DBM indicated incremental axial displacement of the translating gear plate relative to the rotating gear plate at static torques greater than 339 N-m (3000 in-lb). This gear plate "walking" behavior consistently led to complete disengagement at a static torque of 2260 N-m (20,000 in-lb). It was noted that these static torque values were well within the expected range of liftoff and ascent values. The translating gear plate for the outer frame DBM showed no significant motion and never released for the range of applied static torques. The translating gear plate for the inner frame DBM consistently moved when the frequency of the sine sweep reached the fundamental modes of the inner frame structure. The fundamental mode of the outer frame structure was much higher, resulting in a lower force transmitted to the DBM. Therefore, the brake release phenomenon appeared to be a function of displacement caused by an applied axial force and not resonances internal to the DBM.

Phase 1 testing confirmed that static torques and dynamic axial loads are critical to the gear plate "walking" phenomenon. It was apparent that the 8 degree sloped sides of the gear teeth allow the two plates to move in unison when friction at the translating gear plate tangs is overcome. When the applied axial force is reversed, the translating gear plate remains in its displaced position. Figure 6 shows the free body diagram of the translating gear plate and Equation 1 solves for the axial force required to displace this plate. For the translating plate to walk

$$A = T\mu/R2 + S \qquad (1)$$

Where:
- A = axial force
- T = static torque
- S = spring force
- μ = coefficient of friction
- $R2$ = radius at tangs

back, the applied axial force must overcome both the friction force at the tangs, due to static torque, and the preload spring force. If at any time during the dynamic cycle the force along the tooth surface exceeds the friction force, the teeth

slip and motion of the translating gear plate is stopped. Equation 2 can be solved for A to determine the axial force required for the gear teeth to slip. Figure 7 shows the region of brake release as a function of static torque and axial force. The upper line in Figure 7, defined by Equation 1, represents the axial force required to displace the translating gear plate. The lower line, defined by Equation 2, represents the axial force required for the gear teeth to slip.

$$A\mu \sin\alpha + (T\mu/R1) \cos\alpha = A \cos\alpha - (T/R1) \sin\alpha \quad (2)$$

Where: α = tooth angle
R1 = radius at teeth

Measurements were performed to define the axial and torsional stiffness of the inner and outer frame DBMs for both the flight and flight spare units. The axial loads were cycled twice from + to - 17800 N (4000 lb) and the torsional loads were cycled twice from + to - 3390 N-m (30,000 in-lb). The axial load was approximately 70% and the torsional load approximately 20% of the maximum expected flight loads. Stiffness test results showed wide variation of axial and torsional stiffness for each DBM as shown in Figure 8. Note that the critical direction for gear plate disengagement is the negative axial force direction indicated on the plots. These wide variations were caused by a lack of adequate preload on the DBM bearings. It was noted that the DBM which consistently released during Phase 1 testing was also the most flexible in the axial direction. This flexibility allowed the translating gear plate to displace a greater amount during each dynamic load cycle. Axial and torsional dead bands were also measured. The axial dead band was negligible and the torsional dead band or backlash was as expected.

BRAKE LOCK MECHANISM DESIGN

Investigation of the DBM design identified a simple and reliable concept that would increase the preload spring forces in Equation 1. The BLM design incorporates very few moving parts and extremely reliable pyrotechnic pin pullers (Figure 9).

Various options were investigated before settling on the final design. Motor/gear-driven mechanisms, redesigned gear plates and on-orbit relatch capabilities were considered. Motor/gear-driven mechanisms were avoided because of their added complexity and reduced reliability. Gear plate redesigns would require deintegration of the flight-configured payload and disassembly of the flight DBMs. This was considered a noncredible option due to launch schedule constraints. Phase 1 testing identified the magnitude of applied static torque as a determining factor for brake disengagement. It was thought that low static

decelerations during STS descent and landing would not generate the magnitude of static torque necessary to cause brake release. Therefore, an on-orbit relatch capability was not included in the baseline design. This conclusion would be verified during Phase 2 qualification testing.

The original DBM design employed four equally spaced compression springs to preload the translating gear plate against the rotating plate. Both plates had 2.0 mm (0.080 in) deep gear teeth which meshed every 8 degrees. Externally accessible set screws were used to adjust the spring forces to 98 N (22 lb) each for a total preload of 392 N (88 lb). Once on orbit, the solenoid would pull the translating gear plate against the preload springs, releasing the gimbal to rotate. When power was removed, the solenoid was deenergized, and the preload springs reengaged the translating gear plate with the rotating plate.

The BLM design took advantage of the set screw holes to gain access to the translating gear plate without disassembly of the DBM. Two of the four set screws (located 180 degrees apart) were replaced with two phosphor bronze push rod guides having a 3/8-24 external thread and a 4.8 mm (0.188 in) diameter bore through the center. A stainless steel push rod, burnished with a solid film lubricant, was installed in the push rod guide prior to the guide being threaded into the DBM aft housing. The push rods were held in place by pyrotechnic pin pullers which in turn were held in position by an aluminum pin puller bracket that was bolted to the DBM aft housing. Each pin puller bracket was individually shimmed into position so that, when the pin pullers were installed, the push rods compressed the preload springs to about .25 mm (0.010 in) above their solid height.

The solidly compressed springs restrained the translating gear plate and prevented the "walking" action previously observed. Once on orbit, the pin pullers would be fired to release the push rods. The push rod guides were shimmed and set so that after the push rods were released the preload springs would retract to their originally designed positions (392 N preload). When the preload springs were released, the solenoid could be activated, thus retracting the translating gear plate and allowing the gimbal to operate.

For added redundancy, the BLM was made compatible for an Extra Vehicular Activity. If a pin puller failed to fire on orbit, an STS crewmember could release the push rods by loosening three bolts and rotating the bracket until the pin puller no longer contacted the push rod.

FLIGHT LOAD DETERMINATION

Phase 1 testing showed that the brake release phenomenon is sensitive to static torque and dynamic axial loading conditions. Dynamic torques were also included due to their uncertain effect on brake motion. Expected flight loads were

derived for the Phase 2 qualification test program using actual flight data measured on STS-26 and coupled loads analysis data for STS-35. The STS steady state thrust acceleration profile for liftoff and ascent is shown in Figure 10. The steady state thrust reaches a maximum of 1.5 G's during the high dynamic transient liftoff event and approximately 3 G's during main engine cutoff (MECO). The center of gravity of the BBXRT instrument shifts as the argon in the cryogenic coolers at the bottom of the instrument boils off, and can range 12.7 cm (5.0 in) on either side of the instrument center of rotation. This offset center of gravity and steady state thrust acceleration provide a static torque, to the outer frame DBM, during the liftoff and ascent stages of flight. As the static torque increases during ascent, the expected dynamic axial force is reduced. The dynamic axial load is 17800 N (4000 lb) during liftoff with a 1220 N-m (10800 in-lb) static torque. When the steady state thrust load and static torque reach a maximum, the expected dynamic axial load is only 2980 N (670 lb). The inner frame DBM is oriented in the shuttle thrust direction and is subject to high axial loads but insignificant static torques.

STS descent and landing also provide a steady state load environment in the shuttle thrust direction. The maximum steady state deceleration during STS-26 descent and landing was approximately .4 G and occurred after reentry, approximately five minutes before main gear touchdown. The resulting static torque for descent and landing was much lower than the static torque developed during liftoff and ascent; however, it was still high enough at 339 N-m (3000 in-lb) to be a concern. Phase 1 tests showed gear plate motion for this same static torque. A summary of flight load data for the entire flight sequence is shown in Table 1.

BLM QUALIFICATION TESTING

Qualification testing of the BLM was performed at the environmental test facilities of GSFC during August 1989. The purpose of the testing program was to qualify the protoflight BLM units for flight by subjecting the units to the expected flight environment while installed on the flight spare DBMs.

Test Set-up

Physical size limitations of the 1361 kg (3000 lb) flight spare TAPS prevented system-level testing as a complete unit. As a result, each DBM was removed and installed in a test fixture. The test fixture and test set-up are shown in Figure 11. The DBM and test fixture were mounted to the primary (155,700 N/35,000 lb) electrodynamic shaker slip table and a 907 kg (2000 lb) mass simulator was bolted to the DBM drive shaft. The center of gravity of the mass was centered on the drive shaft. A bracket was mounted at one end of the mass to which a bungie

cord was attached. In-line with the bungie, a turnbuckle and crane scale were installed to apply and monitor the static torque. A square tube was welded to the other end of the mass simulator and a 1.8 m (6.0 ft) long shaker stinger was attached. The stinger was attached at the opposite end to an auxiliary (1100 N/250 lb) electrodynamic shaker. The long stinger provided isolation between slip table movement and the auxiliary shaker.

The test fixture was skewed 30 degrees to the primary shaker axis so that sinusoidal acceleration of the 907 kg (2000 lb) mass produced both dynamic axial and shear loads. Static and dynamic torques were applied with the bungie cord and auxiliary shaker, respectively. High levels of dynamic torque were possible by dwelling at the torsional resonance of the DBM drive shaft. Various combinations of dynamic axial loads and dynamic and static torques were simultaneously applied to the DBMs. The test levels were derived from actual flight load data for the entire flight sequence as shown in Table 1. The actual test levels included a 1.25 test factor on all the maximum expected flight levels. The test load cases are presented in Table 2.

Three Linear Variable Differential Transformers (LVDT) were mounted to the DBM aft housing with probes penetrating through the housing and contacting the translating gear plate. The LVDTs measured movement of the translating gear plate relative to the aft housing so that translating gear plate motion could be monitored during the test.

Each BLM push rod was instrumented with two back-to-back uniaxial strain gages. Prior to qualification testing, the push rod/strain gage assemblies were calibrated in compression to indicate load as a function of average strain. During the qualification testing, each back-to-back strain gage pair was averaged and the output force displayed. The push rod loads were monitored very carefully during the test to determine if the induced side loads on the pin pullers would exceed their allowable design limit loads. Seven accelerometers monitored the acceleration of the mass simulator by which the dynamically induced loads could be controlled.

Test Sequence

Prior to installation of the BLM, the DBMs were subjected to the liftoff and ascent load cases shown in Table 2 to demonstrate that at least one of these load cases would cause the brake plates to disengage. After the brake disengaged, it was reset, the BLM was installed and the tests were repeated. Following completion of the liftoff and ascent load cases, a protoflight level random vibration test was performed. The load case causing the most gear plate displacement without the BLM in place was then re-run to obtain a worst case side load on the pin puller. The pin pullers were then fired and the descent/landing load cases run with the preload springs in their as-designed positions. Post-test functional checks were performed to demonstrate that DBM performance requirements were

maintained.

The actual test start-up sequence for each load case began by applying the required static torque. The auxiliary shaker excitation frequency was then manually adjusted from below the DBM drive shaft torsional resonance upward until the excitation frequency was identical to the DBM torsional resonance. Once at resonance, the auxiliary shaker drive current was increased until the desired dynamic torque was attained. High levels of dynamic torque were difficult to attain due to the nonlinearities of the system. When the torsional resonance was dwelled at, and the input level increased, the system would sometimes detune and fall off the resonance, resulting in a drop in the dynamic torque. When the dynamic torque reached an acceptable level, the primary (155,700 N/35,000 lb) electrodynamic shaker was energized. The primary shaker profile was a below resonance sine dwell at 15 hz for 30 seconds and at an appropriate level to achieve the desired dynamic axial force induced by acceleration of the mass simulator.

Test Results

Prior to installing the BLM, high static torque load cases 1A2 and 1A3 resulted in gear plate disengagement on both inner and outer frame DBMs. Typical LVDT responses for this event are shown in Figure 12. With the BLM in place, the translating gear plate was successfully restrained for all liftoff and ascent load cases. Load cases 1A2 and 1A3 caused only 0.5 mm displacement of the translating plate with respect to the rotating plate before the BLM stopped further motion (see Figure 13). Low static torque load case 1A1 caused insignificant displacement of the translating gear plate.

Push rod strain gage data indicated that the maximum side load in the pin puller was only 355 N (80 lb), which is well below the allowable side load of 4000 N (900 lb). After this maximum side load was attained, the pyrotechnic pin pullers were fired, releasing the preload springs to their on-orbit operational position. This completed qualification of the BLM for shuttle liftoff and ascent.

Descent and landing load cases caused insignificant motion of the translating gear plate. Typical LVDT data for these load cases is shown in Figure 14. Since the brake did not disengage during any of the descent and landing load cases, a mechanism to re-lock the gear plates was not required.

Some of the higher levels of dynamic torque were not attainable with the test setup due to the lower than expected amplification factor. The highest target dynamic torque was 20,340 N-m (180,000 in-lb) and the highest level attained was 13,000 N-m (115,000 in-lb). This was acceptable because test results indicated that dynamic torque tended to reseat the translating gear plate.

CONCLUSION AND SUMMARY

Unexpected release of the roll axis brake during the TAPS modal survey testing dictated the need for a design change. A multi-phase recovery plan began with a series of tests to understand the brake failure. Magnitude of static torque and dynamic axial force was identified as a key factor. Simultaneous application of static torque and axial forces to the DBM drive shaft caused the translating gear plate to incrementally displace, or "walk," with respect to the rotating gear plate. Loading conditions that caused the gear plates to separate were representative of the expected flight environment. In parallel with these tests, the BLM was developed to ensure positive gear plate engagement during shuttle liftoff and ascent. Mechanism qualification tests reflected a complex set of simultaneously applied static and dynamic forces to accurately represent the expected flight environment. Without the BLM, the tests consistently demonstrated gear plate walking and eventual disengagement for the high static torque liftoff and ascent load cases. With the BLM in place, the tests conclusively demonstrated that gear plate release was prevented. The translating gear plate showed no significant motion for descent and landing load cases; therefore, a mechanism to re-lock the gear plates was not required.

Analyses and tests performed during execution of the recovery plan resulted in the following lessons learned for future payload and mechanism designs. The wide variation of DBM stiffness measurements was due to inadequate preload on the bearings. Proper bearing preload would not prevent the "walking" phenomenon; however, the displacement of the translating gear plate during each dynamic load cycle would be reduced, which in turn would delay the brake release process. The DBM is a large mechanism located in the primary structural load path. Carrying structural loads through a mechanism that, by definition, is designed to move is not recommended. An improved design would incorporate a true structural load path that could be disabled on orbit to allow normal system operations. Structures are often tested with an equivalent set of loads to represent the combined action of static and dynamic forces. When mechanisms are located in the primary structural load path, verification testing must account for the proper combinations of simultaneously applied static and dynamic loads.

ACKNOWLEDGEMENT

The authors wish to acknowledge and express their appreciation to Ed Devine and Joe O'Connor of Swales and Associates, Inc. for their support and guidance during the design and development of the BLM. Without their invaluable support, it is unlikely that the severe schedule constraint for shipment of the BBXRT payload to the launch site would have been met.

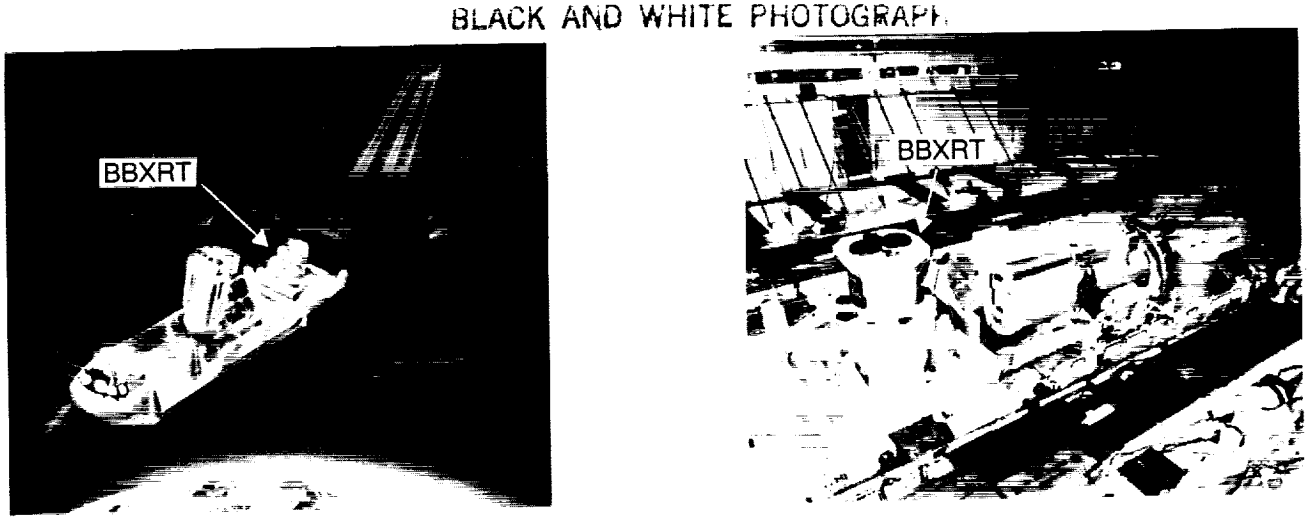

Figure 1 - STS-35 ASTRO-1 Mission

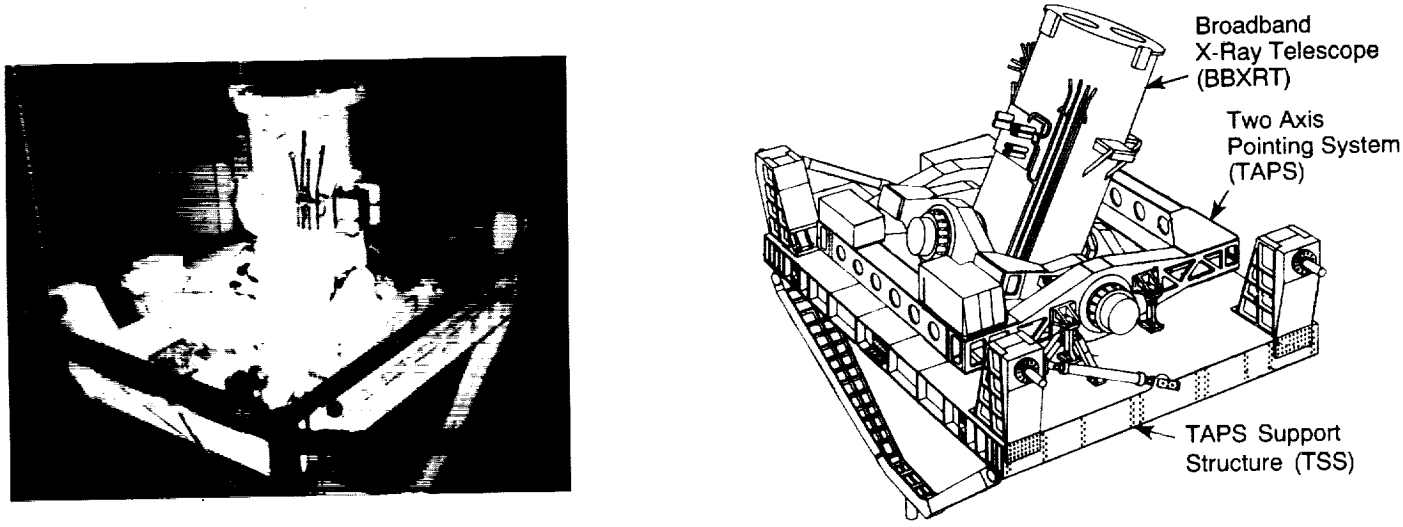

Figure 2 - BBXRT Payload Flight Configuration

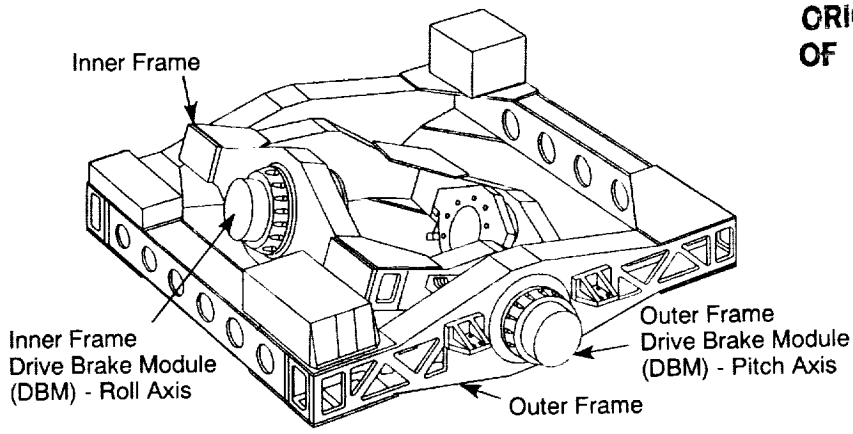

Figure 3 - Two Axis Pointing System (TAPS)

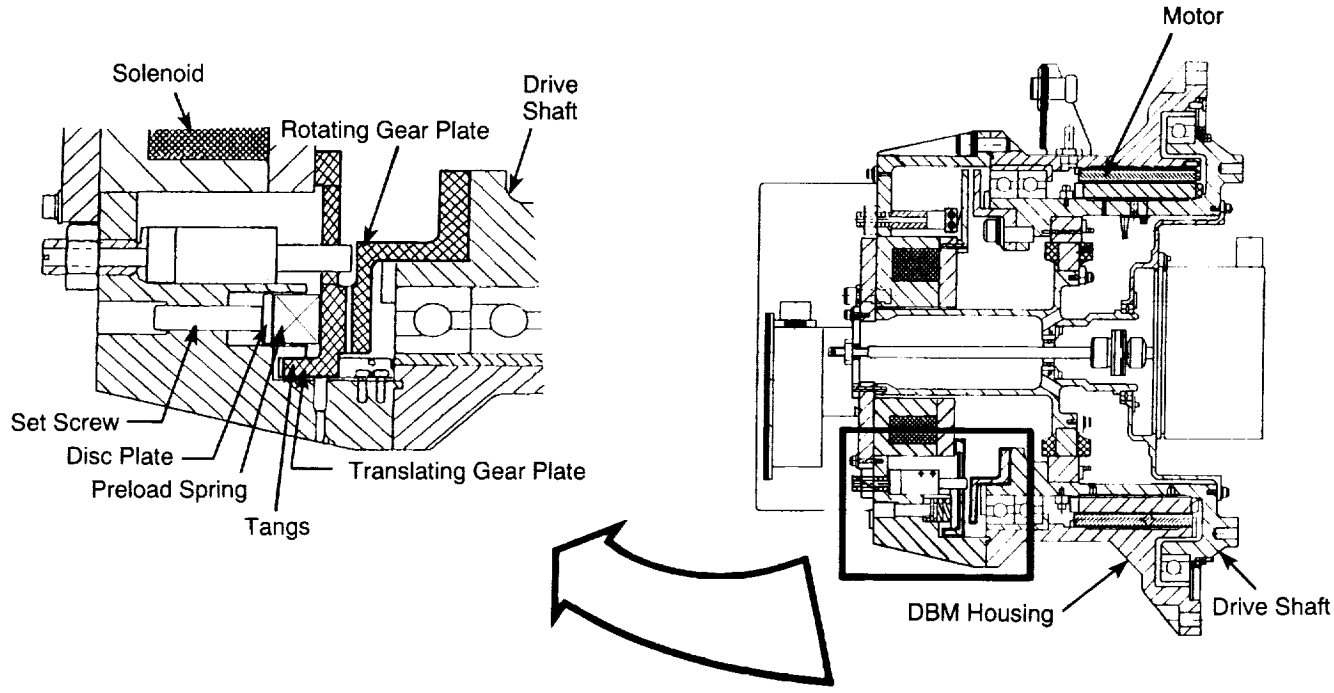

Figure 4 - Drive Brake Module (DBM) Cross Section

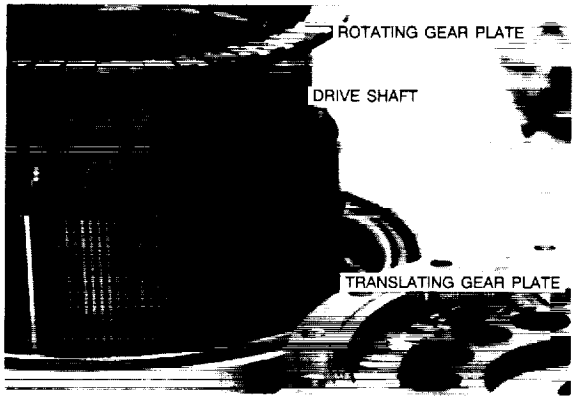

Figure 5 - DBM Translating and Rotating Gear Plates

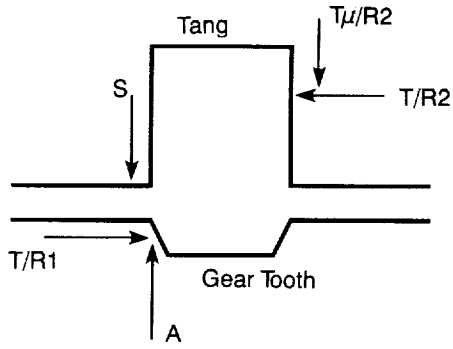

Figure 6 - Free Body Diagram of Translating Gear Plate

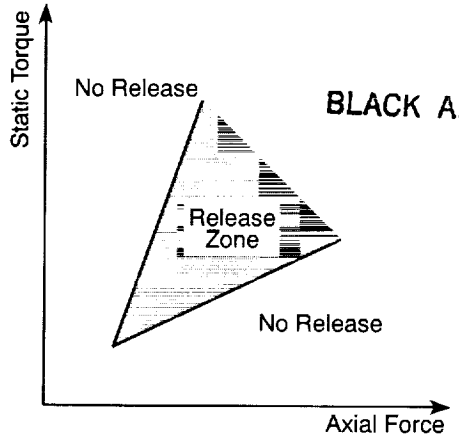

Figure 7 - Gear Plate Release as a Function of Static Torque and Axial Force

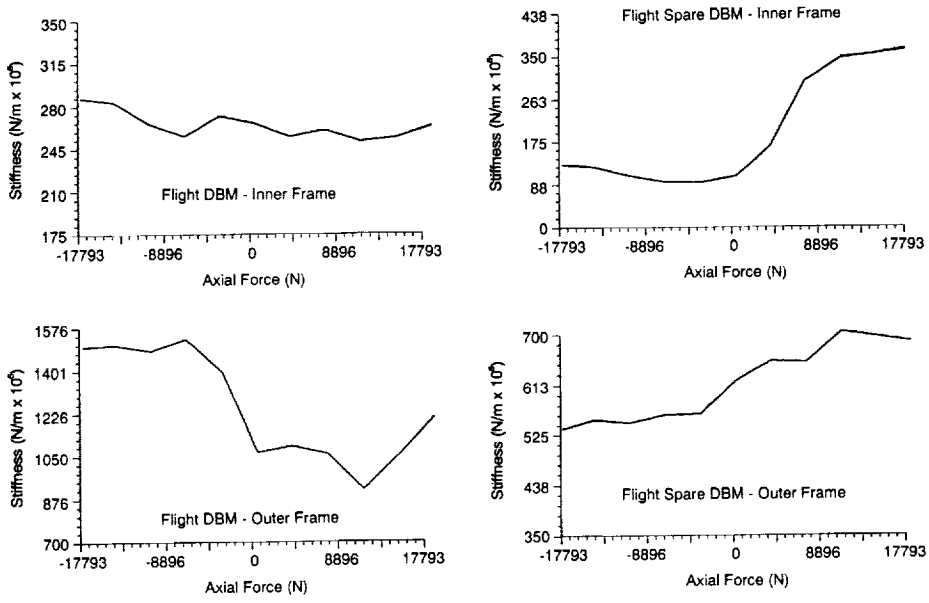

Figure 8 - Results of Drive Brake Module (DBM) Axial Stiffness Measurements

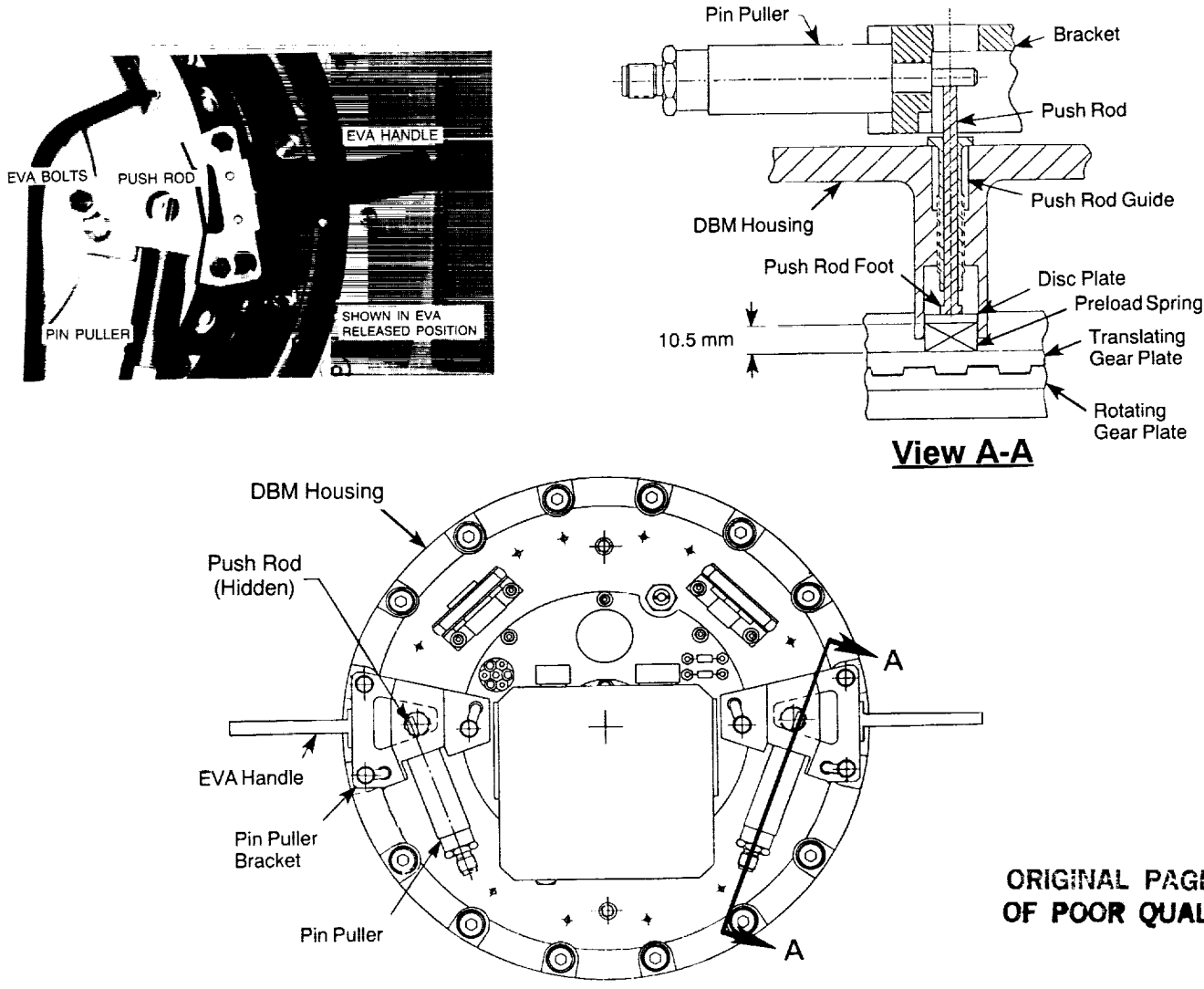

ORIGINAL PAGE IS
OF POOR QUALITY

Figure 9 - Brake Lock Mechanism (BLM)

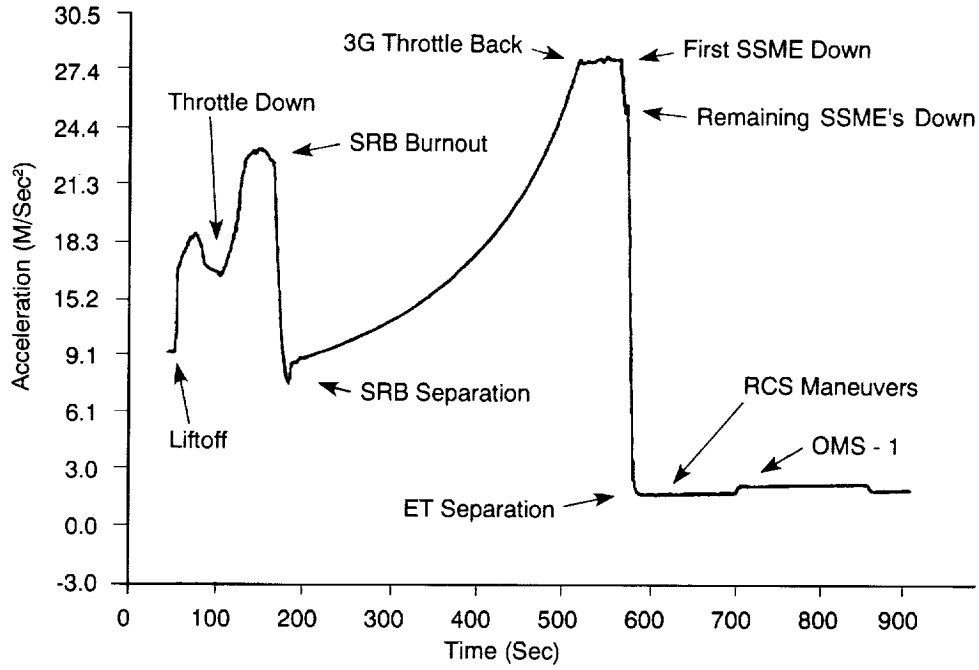

Figure 10 - Steady State Thrust Acceleration Profile for STS Liftoff and Ascent

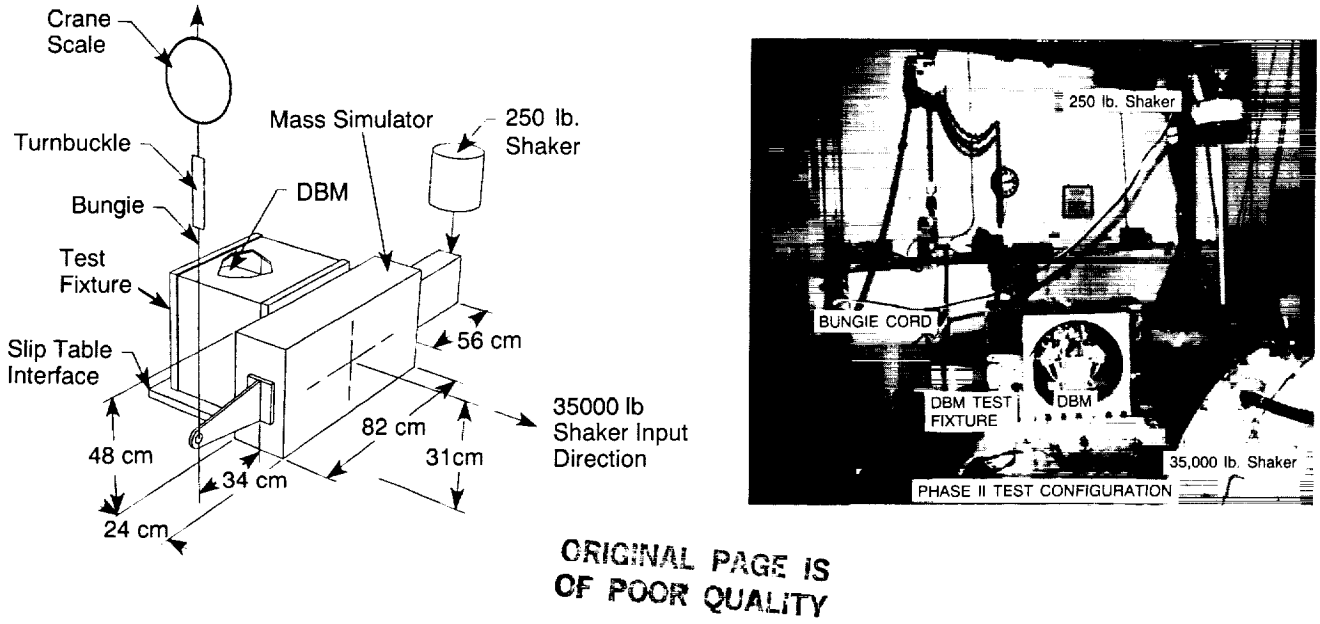

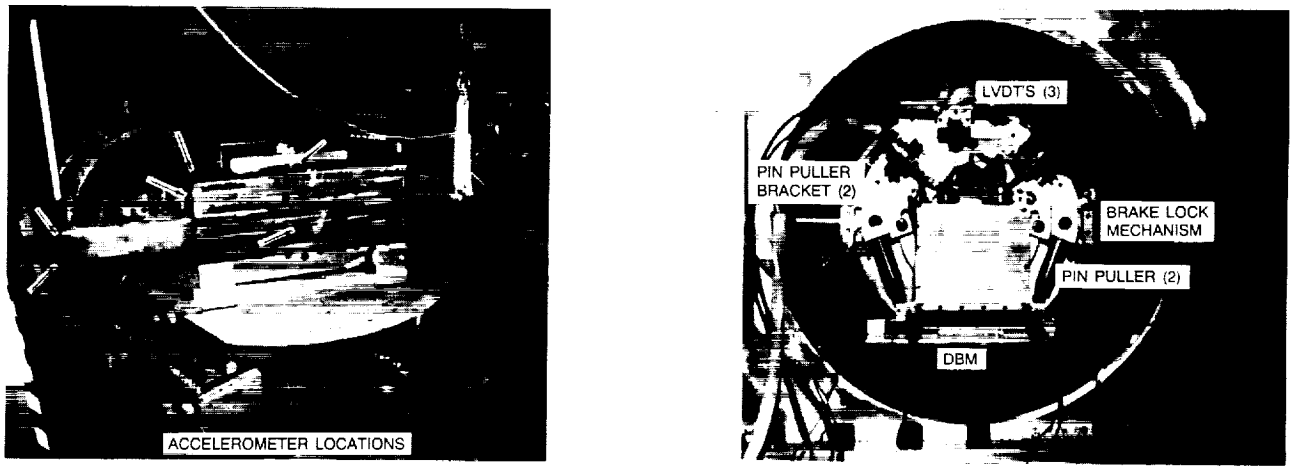

Figure 11 - Phase 2 BLM Qualification Test Configuration

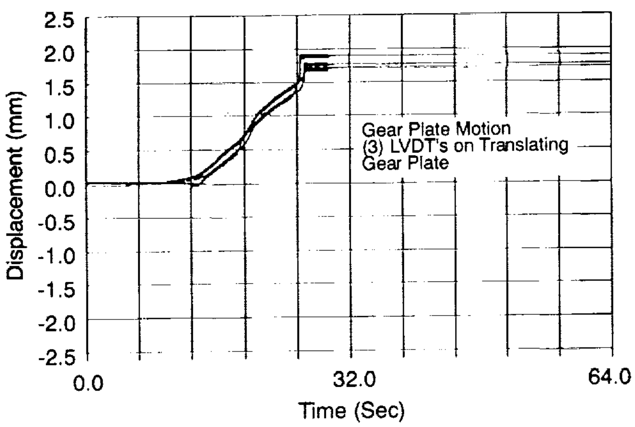

Figure 12 - Translating Gear Plate Displacement for Liftoff and Ascent Load Case 1A3 - Without Brake Lock Mechanism

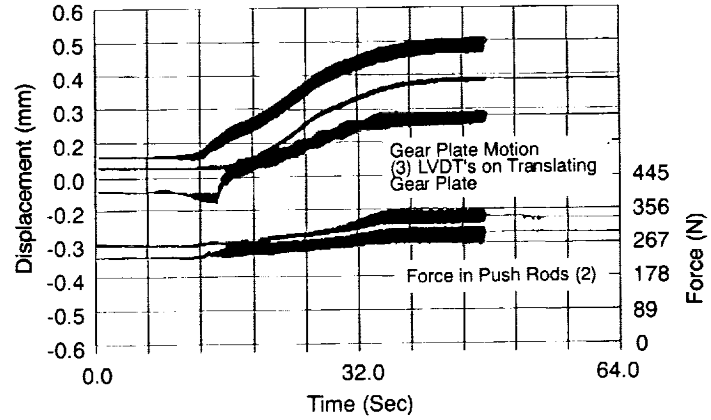

Figure 13 - Translating Gear Plate Displacement and Forces in the Push Rods for Liftoff and Ascent Load Case 1A3 - With Brake Lock Mechanism

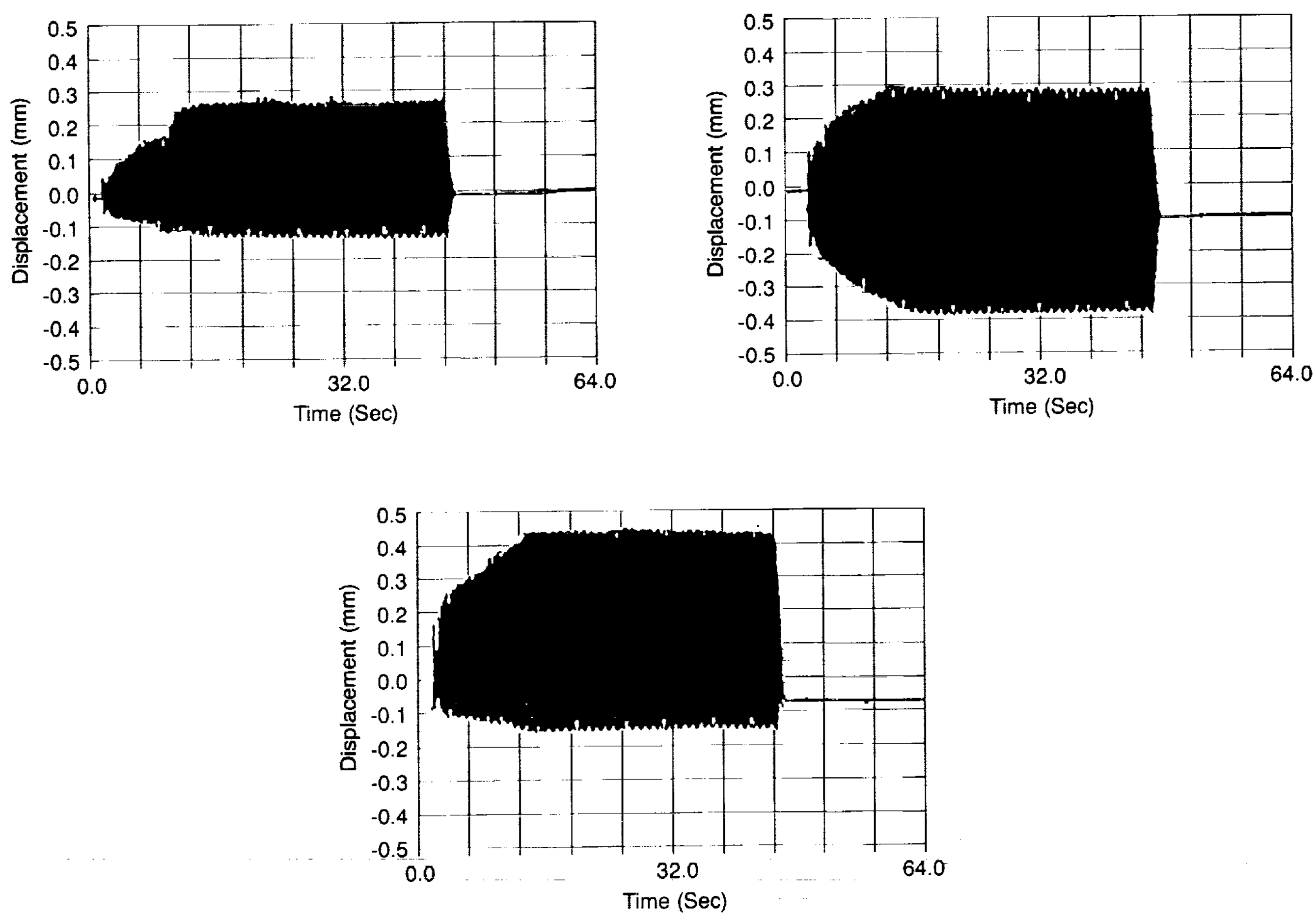

Figure 14 - Translating Gear Plate Displacement for a Typical Descent and Landing Load Case - Without Brake Lock Mechanism

TABLE 1. PREDICTED FLIGHT LOADS FOR TAPS DRIVE BRAKE MODULES (DBM)

EVENT	DBM	STATIC AXIAL (N)	DYNAMIC AXIAL (N)	STATIC TORQUE (N-m)	DYNAMIC TORQUE (N-m)
LIFTOFF	INNER	11565	20905	-	10168
	OUTER	-	17792	1220	14687
MAX. AERO PRESS.	INNER	15123	4893	-	5084
	OUTER	-	8896	1627	3445
MECO	INNER	24464	1423	-	1694
	OUTER	-	2980	2598	870
DECENT	INNER	1868	5782	124	13490
	OUTER	2224	23708	170	3389
LANDING	INNER	3558	38163	-	12428
	OUTER	-	33716	339	12880

TABLE 2. PHASE 2 BLM QUALIFICATION TEST LOAD CASES[1]

LOAD CASE NO.	DYNAMIC AXIAL (N)	STATIC TORQUE (N-m)	DYNAMIC TORQUE (N-m)
LIFTOFF/ASCENT			
1A1	22241	825	0
1A2	22241	1649	0
1A3	22241	2062	0
1B1	22241	825	9185
1B2	22241	1649	9185
1B3	22241	2062	9185
1C1	22241	825	17965
1C2	22241	1649	17965
1C3	22241	2062	17965
2A1	3736	1300	0
2A2	3736	2598	0
2A3	3736	3248	0
2B1	3736	1300	1059
2B2	3736	2598	1059
2B3	3736	3248	1059
DECENT/LANDING			
3A	47596	0	0
3B	47596	0	7773
3C	47596	0	15535
4A	42169	410	0
4B	42169	410	10168
4C	42169	410	20337

[1] These levels include a 1.25 test factor